Electronic Supplementary Material (ESI) for Dalton Transactions.

Two Derivatives of Phenylpyridyl-fused Boroles with Contrasting Electronic Properties: Decreasing and Enhancing the Electron Accepting Ability

Jiang He, Florian Rauch, Ivo Krummenacher, Holger Braunschweig, Maik Finze,* and Todd B. Marder*

[*]Institute for Inorganic Chemistry and Institute for Sustainable Chemistry & Catalysis with Boron (ICB), Julius-Maximilians-Universität Würzburg, Am Hubland, 97074 Würzburg (Germany)

Email: maik.finze@uni-wuerzburg.de

todd.marder@uni-wuerzburg.de

General information

All starting materials were purchased from commercial sources and used without further purification or prepared following reported procedures. All solvents for synthetic reactions and for photophysical and electrochemical measurements were HPLC grade, further treated to remove trace water using an Innovative Technology Inc. Pure-Solv Solvent Purification System and deoxygenated using the freeze-pump-thaw method. All synthetic reactions were performed in an Innovative Technology Inc. glovebox or under an argon atmosphere using standard Schlenk techniques.

General characterization

^{1}H, ^{13}C{^{1}H}, ^{11}B{^{1}H}, ^{19}F{^{1}H}, ^{1}H-^{15}N heteronuclear correlation and ^{1}H-^{1}H NOESY NMR spectra were measured at 298 K using a Bruker Avance I 500 MHz (^{1}H, 500 MHz; ^{13}C, 125 MHz; ^{11}B, 160 MHz) or Bruker Avance III 400 MHz (^{1}H, 400 MHz; ^{13}C, 101 MHz; ^{11}B, 128 MHz; ^{19}F, 376 MHz) NMR spectrometer. Chemical shifts (δ) were referenced to solvent peaks as follows: ^{1}H NMR spectra were referenced to residual $CHCl_3$ in $CDCl_3$ (7.26 ppm), CD_2Cl_2 (5.32 ppm), d_8-THF (1.72 and 3.58 ppm) or d_6-DMSO (2.50 ppm); ^{13}C{^{1}H} NMR spectra were referenced to $CDCl_3$ (77.16 ppm), CD_2Cl_2 (53.84 ppm) or d_6-DMSO (39.52 ppm); ^{11}B{^{1}H} NMR signals were referenced to external $BF_3{\cdot}OEt_2$ and ^{19}F{^{1}H} NMR signals were referenced to $CFCl_3$. Elemental analyses were performed on an Elementar vario MICRO cube elemental analyzer in our institute. Elemental analyses were performed on an Elementar vario MICRO cube elemental analyzer in our Institute. Carbon analysis of compound **1** was up to 1.4% below the calculated value, while hydrogen and nitrogen were satisfactory. This may be ascribed to the formation of boron carbide.[1] Due to the instability and high percentage weight of fluorine atoms weight (10.72%), the elemental analysis of compound **2** was not measured. High resolution mass spectrometry (HRMS) was performed with a Thermo Fisher Scientific Exactive Plus Orbitrap MS System with either an atmospheric pressure chemical ionization (APCI) or a heated-electrospray ionization (HESI) probe.

Photophysical measurements

All measurements were performed under an argon atmosphere with a standard quartz cuvette (1 cm × 1 cm cross-section). UV-visible absorption spectra were recorded using a LAMBDA 465 diode array UV-visible spectrophotometer. Molar extinction coefficients were calculated from three independently prepared samples. Excitation and emission spectra were recorded using an Edinburgh Instruments FLSP920 spectrometer equipped with a double monochromator for both excitation and emission, operating in right-angle geometry mode, and all spectra were fully corrected for the spectral response of the instrument. The concentrations of all the solutions were lower than 10^{-5} M (for **1**) or ca. 2×10^{-5} M (for **2**) to minimize inner filter effects during fluorescence measurements.

Fluorescence quantum yield measurements

Fluorescence quantum yields were measured using a calibrated integrating sphere (150 mm inner diameter) from Edinburgh Instruments combined with the FLSP920 spectrometer described above.

Lifetime measurements

Fluorescence lifetimes were recorded via the time-correlated single photon counting (TCSPC) method using an Edinburgh Instruments FLS920 spectrometer equipped with a high-speed photomultiplier tube positioned after a single emission monochromator. Measurements were made in right-angle geometry mode, and the emission was collected through a polarizer set to the magic angle. Both compounds were excited with pulsed diode lasers at wavelengths of 377 nm at repetition rates of 10 or 0.5 MHz, respectively. The full-width-at-half-maximum (FWHM) of the pulse from the diode laser was ca. 90 ps with an instrument response function (IRF) of ca. 1 ns FWHM, respectively. The IRFs were measured from the scatter from pure $BaSO_4$. Decays were recorded to 10000 counts in the peak channel with a record length of at least 1000 channels. The band pass of the emission monochromator and a variable neutral density filter on the excitation side were adjusted to give a signal count rate of

<60 kHz. Iterative reconvolution of the IRF with one decay function and non-linear least-squares analysis were used to analyze the data. The quality of decay fits was judged to be satisfactory based on the calculated values of the reduced χ^2 and Durbin-Watson parameters and visual inspection of the weighted residuals.

Electrochemical measurements

Cyclic voltammetry experiments were performed using a Gamry Instruments Reference 600 potentiostat. A standard three-electrode cell configuration was employed using a platinum disk working electrode, a platinum wire counter electrode, and a silver wire, separated by a *Vycor* tip, serving as the reference electrode. Formal redox potentials are referenced to the ferrocene/ferrocenium redox couple. Tetra-*n*-butylammonium hexafluorophosphate ([*n*-Bu_4N][PF_6]) was employed as the supporting electrolyte. Compensation for resistive losses (*iR* drop) was employed for all measurements.

Theoretical studies

All calculations (DFT and TD-DFT) were carried out with the Gaussian 16 (16.A.03)[2] program package and were performed on a parallel cluster system. GaussView (6.0.16), Avogadro (1.2.0)[3] and multiwfn[4] were used to visualize the results, to measure calculated structural parameters, and to plot orbital surfaces (isovalue: ± 0.030 [e a_0^{-3}]$^{1/2}$). The ground-state geometries were optimized using the B3LYP functional[5] in combination with the 6-31+G(d, p) basis set.[6] The ultrafine integration grid and no symmetry constraints were used for all molecules. Frequency calculations were performed on the optimized structures to confirm them to be local minima showing no negative (imaginary) frequencies. Based on these optimized structures, the lowest-energy vertical transitions (gas-phase) were calculated (singlets, 25 states) by TD-DFT, using B3LYP in combination with the 6-31+G(d, p) basis set (**1**) or CAM-B3LYP in combination with the 6-31++G(d, p) basis set (**2**).[6] NICS values were calculated at the B3LYP/6-311+G(d, p) level of theory.

Synthesis

3-(*Tert*-butyl)-9-(2,4,6-tri*iso*propylphenyl)-3,9-dihydro-2H-benzo[4,5]borolo[2,3-c]pyridine (1)

To a solution of 3-bromo-4-(2-bromophenyl)pyridine[7] (626 mg, 2 mmol) in THF (30 mL), ^{n}BuLi (2 mmol) was added at –78 °C. The resulting solution was stirred at –78 °C for 1 h then $B(OMe)_3$ (4 mmol, 0.44 mL) was added. The reaction was allowed to warm to r.t. and was stirred at r.t. for 6 h. The volatiles were removed under vacuum and the residue was extracted with CH_2Cl_2 (2 × 5 mL). The CH_2Cl_2 was removed under vacuum and the resulting solid was dissolved in THF (15 mL) and cooled to 0 °C. TipMgBr (2 mmol)[8] was added at 0 °C and then the mixture was warmed to 75 °C for 3 h. After cooling to r.t. and stirring for another 6 h, the volatiles were removed under vacuum. The resulting solid was extracted with hexane and then the hexane was removed under vacuum. The crude ^{1}H NMR spectrum indicated a ca. 50% yield of product had formed (the side products are $TipB(OMe)_2$ and 1,3,5-tri*iso*propylbenzene, and the yield is based on the integration of aromatic protons of the Tip group among these three compounds). Then, the light yellow oil was dissolved in THF, cooled to –78 °C, and ^{t}BuLi (2.0 eq, 2 mmol) was added. The mixture was stirred at –78 °C for 2 h and then slowly warmed to r.t. and stirred at r.t for another 6 h. The volatiles were removed again and the residue was extracted with CH_2Cl_2 (2 × 5 mL). The solution was concentrated, hexane was added, and cooling to –30 °C gave compound **1** in 10% yield (86 mg) as a light yellow solid. ^{1}H NMR (500 MHz, $CDCl_3$, ppm): *δ* 7.76-7.72 (m, 1H), 7.58-7.54 (m, 1H), 7.44 (dt, *J* = 7, 1 Hz, 1H), 7.34-7.31 (m, 1H), 7.26 (dt, *J* = 7, 1 Hz, 1H), 7.01-6.96 (m, 2H), 6.00-5.96 (m, 1H), 5.17-5.06 (m, 1H), 4.01 (dd, *J* = 4, 2 Hz, 1H), 2.93 (sept, *J* = 7 Hz, 1H), 2.65 (sept, *J* = 7 Hz, 1H), 2.63 (sept, *J* = 7 Hz, 1H), 1.31 (d, *J* = 7 Hz, 6H), 1.12 (d, *J* = 7 Hz, 3H), 1.10-1.06 (m, 9H), 0.99 (s, 1H); ^{13}C{^{1}H} NMR (125 MHz, $CDCl_3$, ppm): *δ* 150.7, 150.5, 149.7 (br), 148.4, 147.5, 147.4, 143.1, 136.6 (br), 132.3, 130.2, 127.5, 120.2, 119.6, 119.5, 113.1 (br), 104.4, 62.7, 38.6, 34.9, 34.8, 34.3, 34.28, 25.3, 25.0, 24.9, 24.8, 24.3, 24.27, 24.25; ^{11}B{^{1}H} NMR (160 MHz, $CDCl_3$, ppm): *δ* 58.8 (br). HRMS (APCI^{+}): m/z calcd for $[C_{30}H_{40}BN+H]^{+}$: 426.3327; Found: 426.3318 $[M+H]^{+}$; Elem. Anal. Calcd (%) for $C_{30}H_{40}BN$: C, 84.69; H, 9.48; N, 3.29; Found: C,

83.28; H, 9.58; N, 3.11.

1-Methyl-5-(2,4,6-tri*iso*propylphenyl)-5*H*-benzo[4,5]borolo[3,2-b]pyridin-1-ium triflate (2)

To a solution of **TipPBB2** (74 mg, 0.2 mmol) in CH_2Cl_2 (2.0 mL), MeOTf (30 mg, 0.2 mmol) in 0.5 mL CH_2Cl_2 was added at –30 °C. The resulting solution was warmed to r.t. and stirred at r.t. for 3 h. Hexane (ca. 6 mL) was added and the mixture was concentrated under vacuum until a yellow solid precipitated. The solid was collected by filtration, washed with ca. 20 mL of hexane, and dried under vacuum. Compound **2** was obtained in 39% yield (40 mg) as a yellow solid. ^{1}H NMR (400 MHz, CD_2Cl_2, ppm): *δ* 8.78-8.67 (m, 1H), 8.23-8.13 (m, 1H), 8.09-7.99 (m, 1H), 7.80-7.71 (m, 2H), 7.71-7.64 (m, 1H), 7.64-7.54 (m, 1H), 7.10 (s, 2H), 4.67 (s, 3H), 2.95 (sept, *J* = 7 Hz, 1H), 2.27 (sept, *J* = 7 Hz, 2H), 1.30 (d, *J* = 7 Hz, 6H), 1.17-1.09 (m, 12H); ^{13}C{^{1}H} NMR (100 MHz, CD_2Cl_2, ppm): *δ* 166.7, 151.7, 151.1, 149.1, 147.6, 143.6, 137.9, 137.1, 135.1, 128.0, 127.2, 121.4, 48.3, 37.6, 34.9, 25.0, 24.9, 24.1; ^{11}B{^{1}H} NMR (128 MHz, CD_2Cl_2, ppm): *δ* 72.3 (br); ^{19}F{^{1}H} NMR (376 MHz, CD_2Cl_2, ppm): *δ* –79.0. HRMS (ESI$^+$): m/z calcd for $[C_{27}H_{33}BN]^+$: 382.2701; Found: 382.2692 $[M]^+$; HRMS (ESI$^-$): m/z calcd for $[CF_3O_3S]^-$: 148.9526; Found: 148.9519 $[M]^-$.

1-Methyl-2-phenylpyridin-1-ium triflate (3)[9]

To a solution of 2-phenylpyridine (78 mg, 0.5 mmol) in CH_2Cl_2 (2.0 mL), MeOTf (82 mg, 0.5 mmol) in 0.5 mL CH_2Cl_2 was added at –30 °C. The resulting solution was warmed to r.t. and stirred at r.t. for 3 h. The solvent was removed under reduced pressure, the resulting residue was washed with Et_2O in an ultrasonic bath. A white sold was obtained in 58% (92 mg) yield. ^{1}H NMR (400 MHz, DMSO, ppm): *δ* 9.17-9.09 (m, 1H), 8.68-8.59 (m, 1H), 8.19-8.12 (m, 1H), 8.11-8.06 (m, 1H), 7.73-7.62 (m, 5H), 4.12 (s, 3H); ^{13}C{^{1}H} NMR (100 MHz, DMSO, ppm): *δ* 155.0, 146.7, 145.4, 131.8, 131.1, 129.8, 129.2, 129.1, 126.6, 120.7 (q, *J* = 322 Hz), 47.1; ^{19}F{^{1}H} NMR (376 MHz, DMSO, ppm): *δ* –77.7. HRMS (ESI$^+$): m/z calcd for $[C_{12}H_{12}N]^+$: 170.0964; Found: 170.0961 $[M]^+$; HRMS (ESI$^-$): m/z calcd for $[CF_3O_3S]^-$: 148.9526; Found: 148.9513 $[M]^-$.

The data nicely matches that previously reported.[9]

Determination of the selectivity of bromine-lithium exchange reaction: For convenience of purification, we transformed the air sensitive compound **4** into air stable compound **5**.

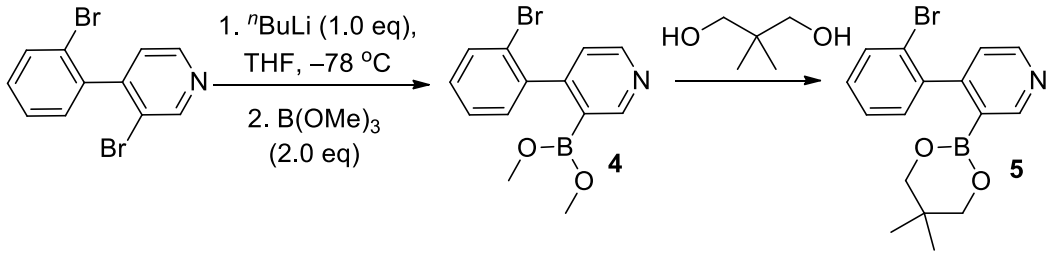

4-(2-Bromophenyl)-3-(5,5-dimethyl-1,3,2-dioxaborinan-2-yl)pyridine (5)

To a solution of 3-bromo-4-(2-bromophenyl)pyridine[7] (313 mg, 1 mmol) in THF (15.0 mL), ^{n}BuLi (1 mmol) was added at –78 °C. The resulting solution was stirred at –78 °C for 1 h then $B(OMe)_3$ (2 mmol, 0.22 mL) was added. The reaction was allowed to warm to r.t. and stirred at r.t. for 6 h. The compound 2,2-dimethylpropane-1,3-diol (3 mmol) was added and the reaction was stirred at r.t. for another 6 h. All volatiles were removed under vacuum and the residue was extracted with hexane. Then the hexane was removed under vacuum and compound **5** was obtained as a white solid in 81% (280 mg) yield. ^{1}H NMR (500 MHz, $CDCl_3$, ppm): δ 8.96 (d, J = 1 Hz, 1H), 8.65 (d, J = 5 Hz, 1H), 7.62-7.58 (m, 1H), 7.36-7.31 (m, 1H), 7.23-7.18 (m, 2H), 7.12 (dd, J = 5, 1 Hz, 1H), 3.52 (s, 2H), 3.51 (s, 2H), 0.92 (s, 6H); ^{13}C{^{1}H} NMR (125 MHz, CD_2Cl_2, ppm): δ 154.8, 154.4, 150.6, 142.2, 132.2, 130.2, 129.0, 126.9, 124.14, 122.4, 72.4, 31.8, 22.0; ^{11}B{^{1}H} NMR (160 MHz, $CDCl_3$, ppm): δ 26.8. HRMS (APCI^{+}): m/z calcd for $[C_{16}H_{17}BBrNO_2+H]^{+}$: 346.0608; Found: 346.0602 $[M+H]^{+}$; Elem. Anal. Calcd (%) for $C_{16}H_{17}BBrNO_2$: C, 55.54; H, 4.95; N, 4.05; Found: C, 55.12; H, 5.00; N, 3.71.

NMR spectra

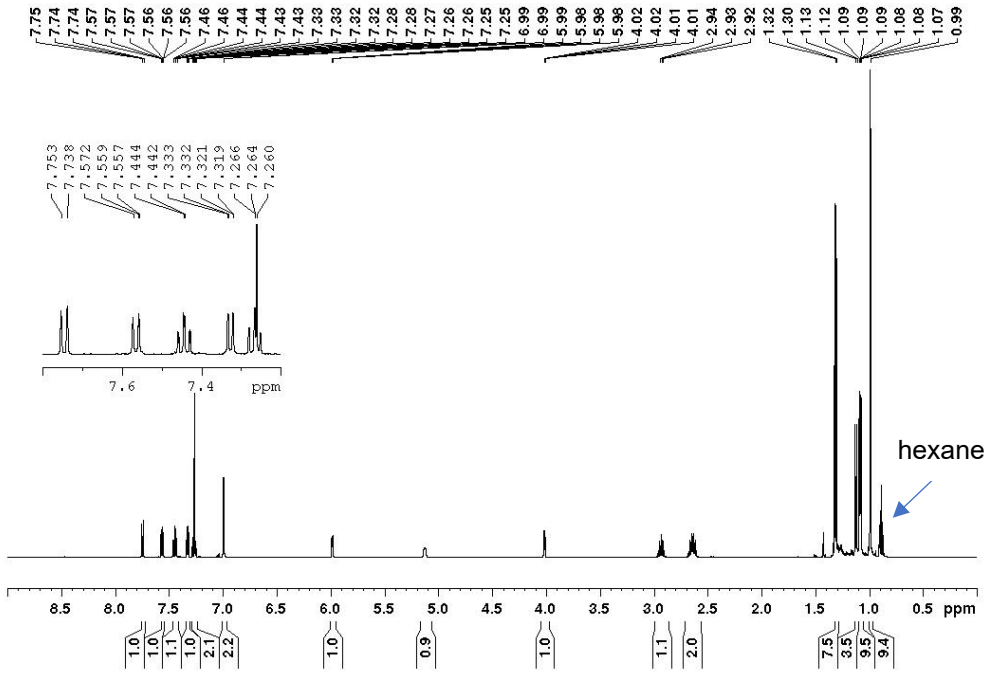

Figure S1. ^{1}H NMR spectrum of compound **1** in $CDCl_3$ at 500 MHz.

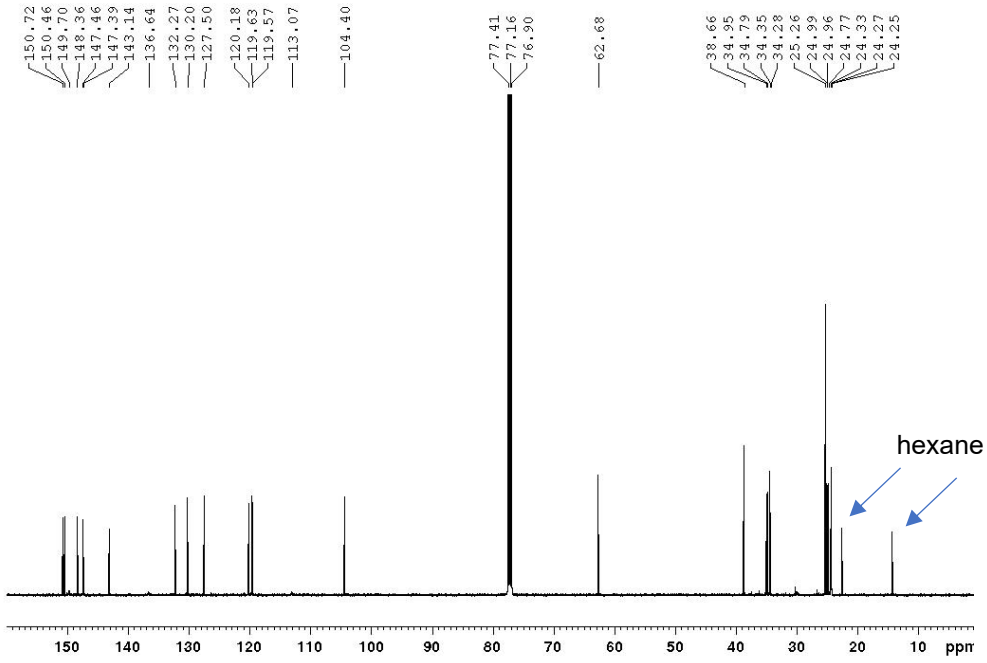

Figure S2. $^{13}C\{^{1}H\}$ NMR spectrum of compound **1** in $CDCl_3$ at 125 MHz.

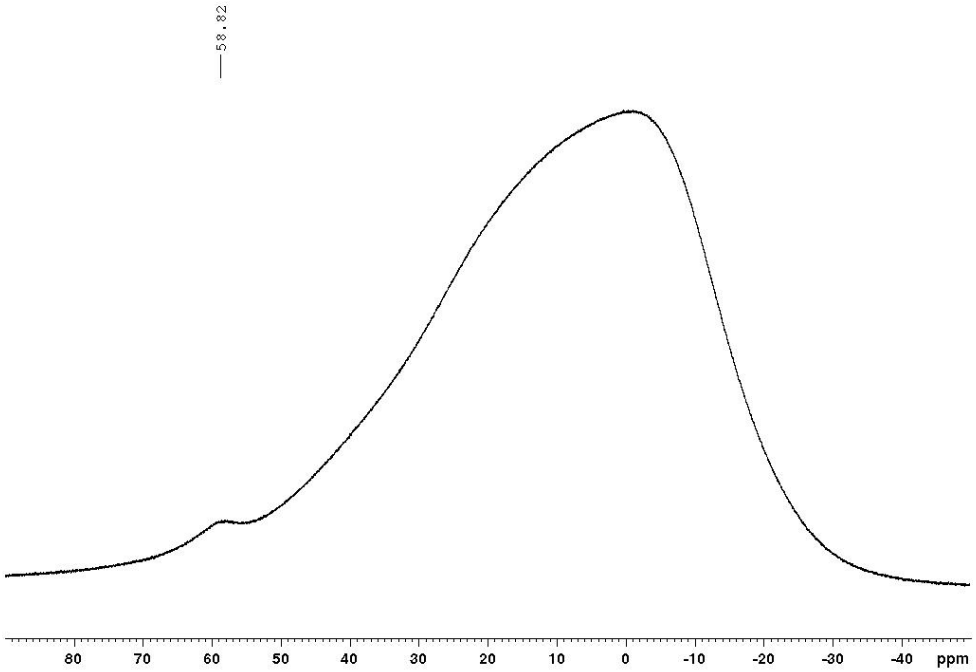

Figure S3. $^{11}B\{^{1}H\}$ NMR spectrum of compound **1** in $CDCl_3$ at 160 MHz.

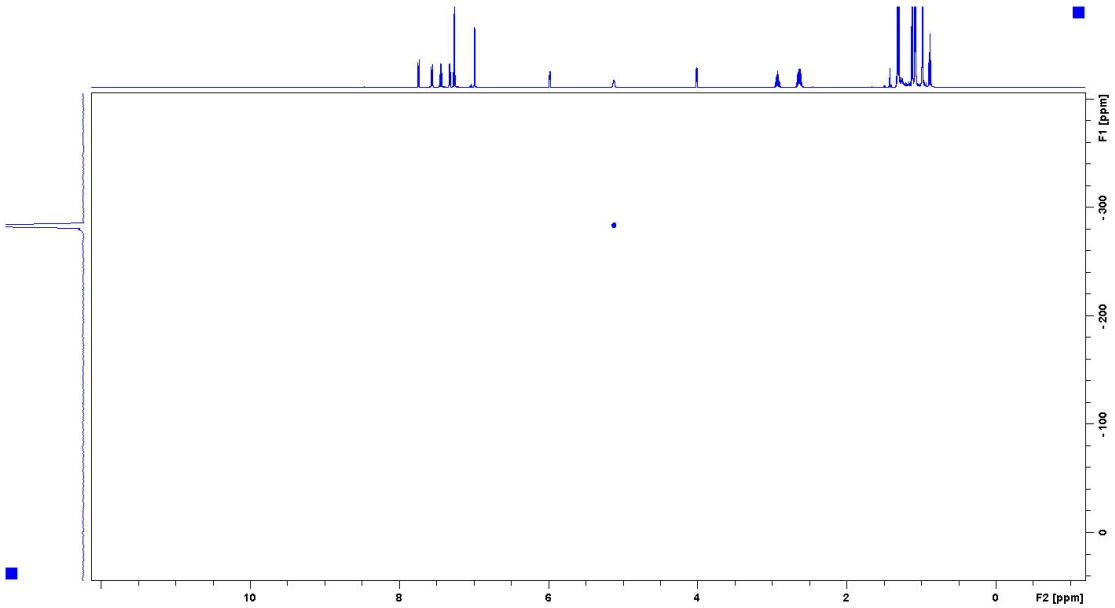

Figure S4. ^{1}H-^{15}N heteronuclear correlation NMR spectrum of compound **1** in $CDCl_3$.

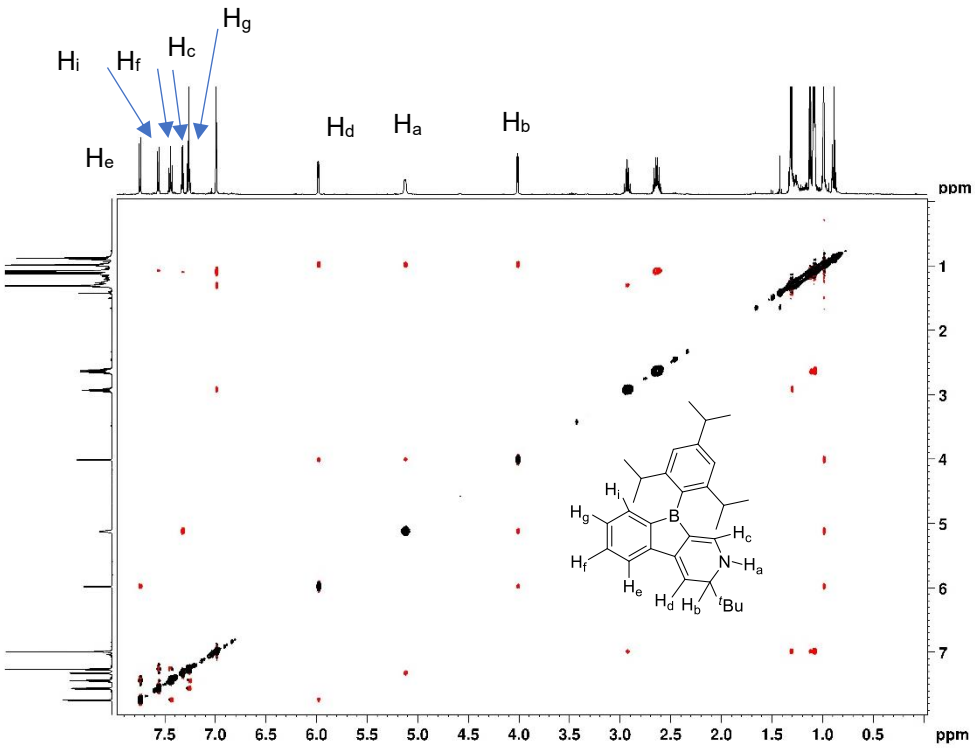

Figure S5. ^{1}H-^{1}H NOESY NMR spectrum of compound **1** in $CDCl_3$ at 500 MHz.

From ^{1}H-^{15}N heteronuclear correlation, we can assign the chemical shift of proton H_a (5.17-5.06 ppm). H_a is coupled to both H_b and H_c, but H_c only couples with H_a. Thus, H_c can be assigned (7.34-7.31 ppm). After H_c was assigned, H_b (4.01 ppm) was also assigned. H_b also couples with H_d, thus H_d was assigned with a chemical shift of 6.00-5.96 ppm. As H_d has an NOE effect with H_e, H_e can be assigned and the other three protons (H_f, H_g and H_i) were assigned in the same way through coupling.

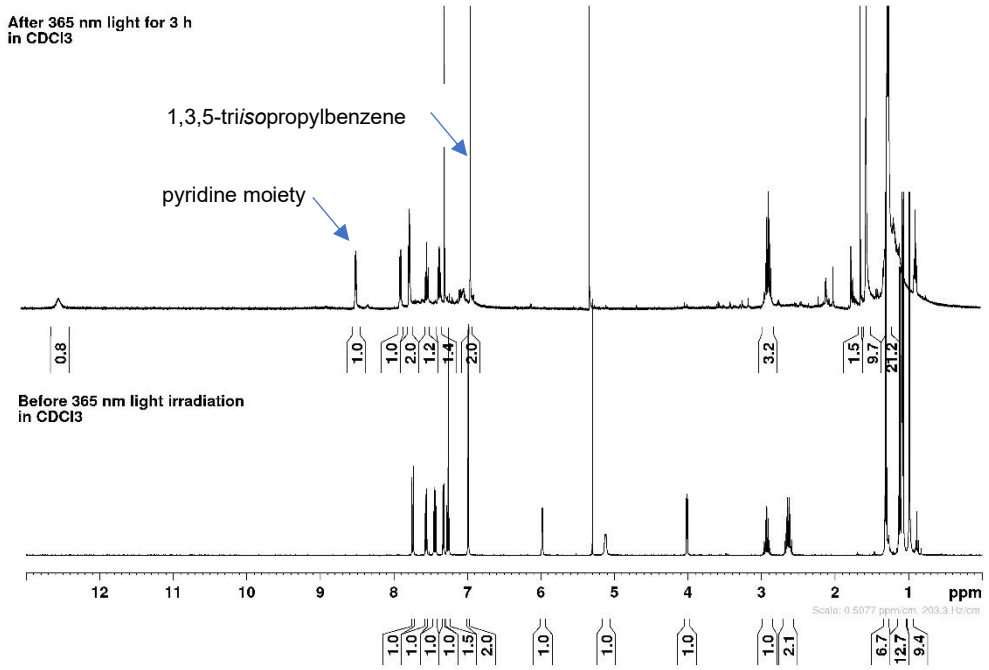

Figure S6. ^{1}H NMR spectra of compound **1** in $CDCl_3$ before (bottom) and after 365 nm light (top) at 400 MHz.

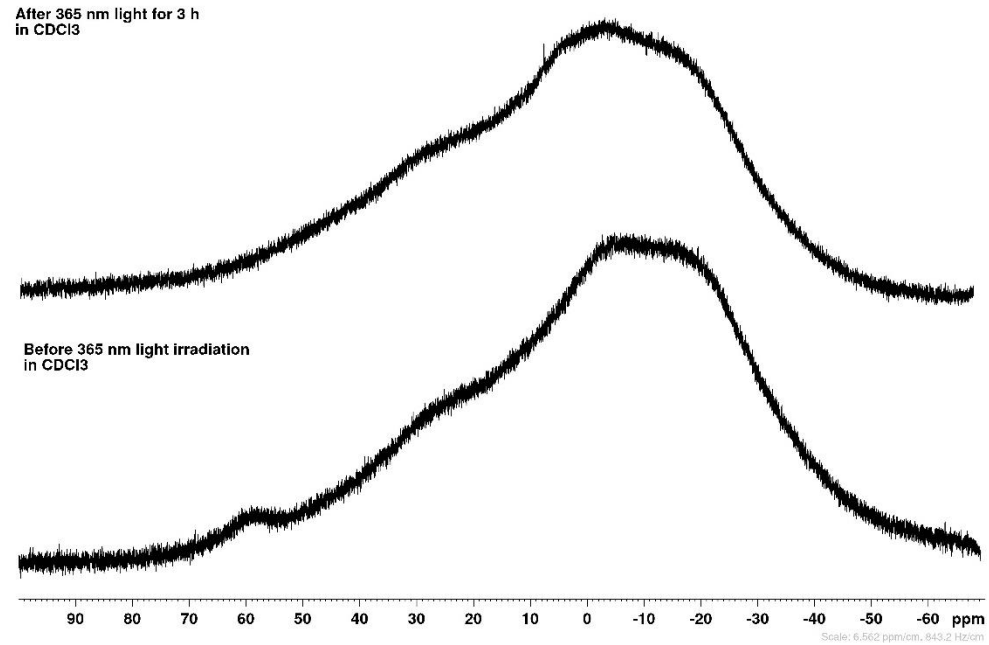

Figure S7. $^{11}B\{^{1}H\}$ NMR spectra of compound **1** in $CDCl_3$ before (bottom) and after 365 nm light (top) at 128 MHz.

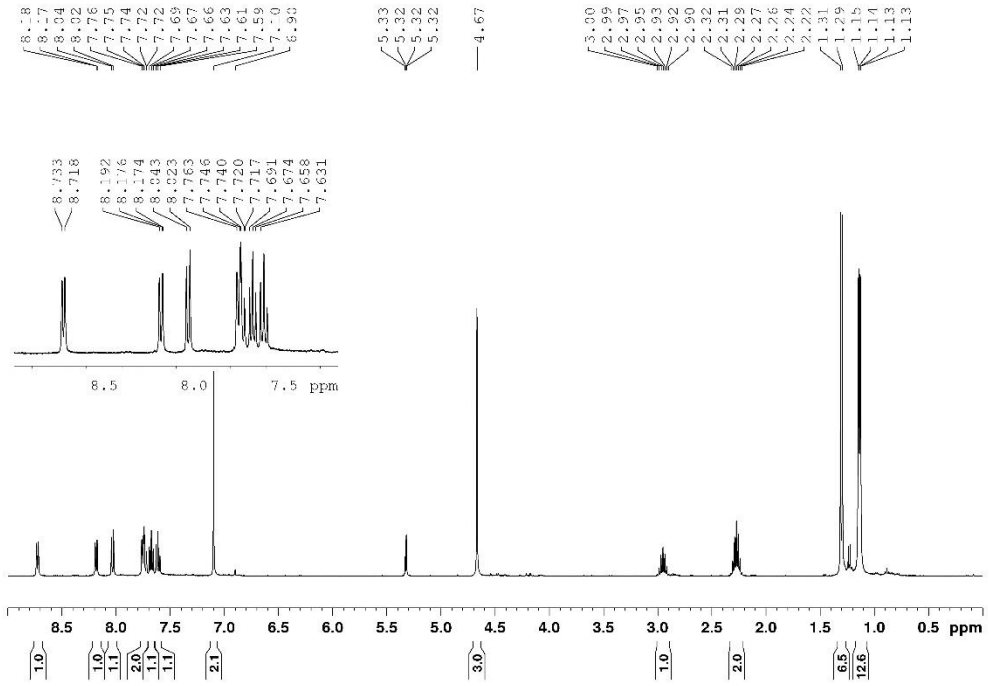

Figure S8. ^{1}H NMR spectrum of compound **2** in CD_2Cl_2 at 400 MHz.

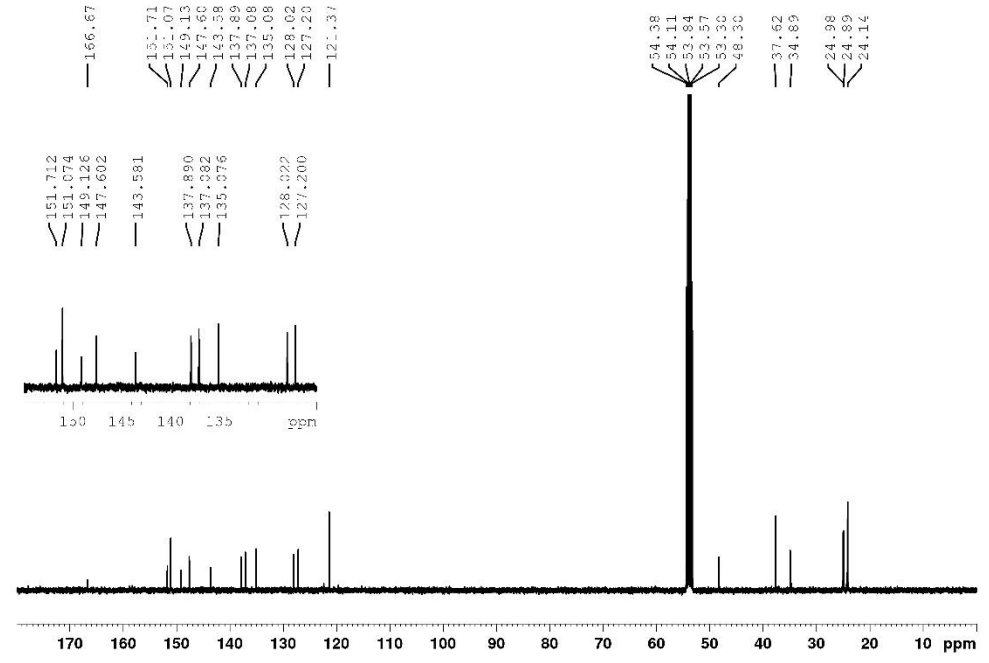

Figure S9. $^{13}C\{^{1}H\}$ NMR spectrum of compound **2** in CD_2Cl_2 at 100 MHz.

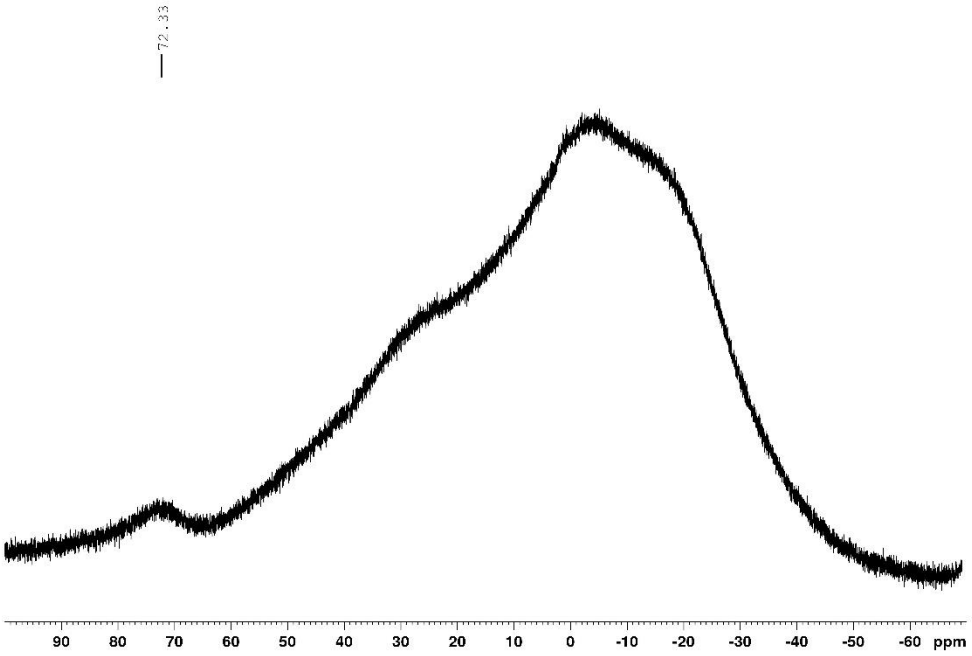

Figure S10. $^{11}B\{^{1}H\}$ NMR spectrum of compound **2** in CD_2Cl_2 at 128 MHz.

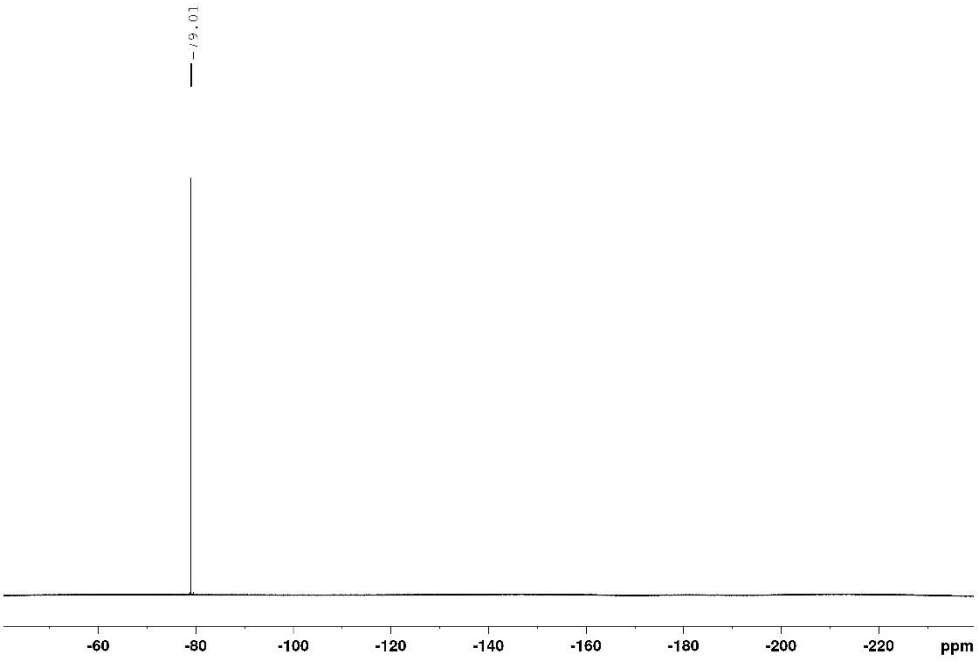

Figure S11. $^{19}F\{^{1}H\}$ NMR spectrum of compound **2** in CD_2Cl_2 at 376 MHz.

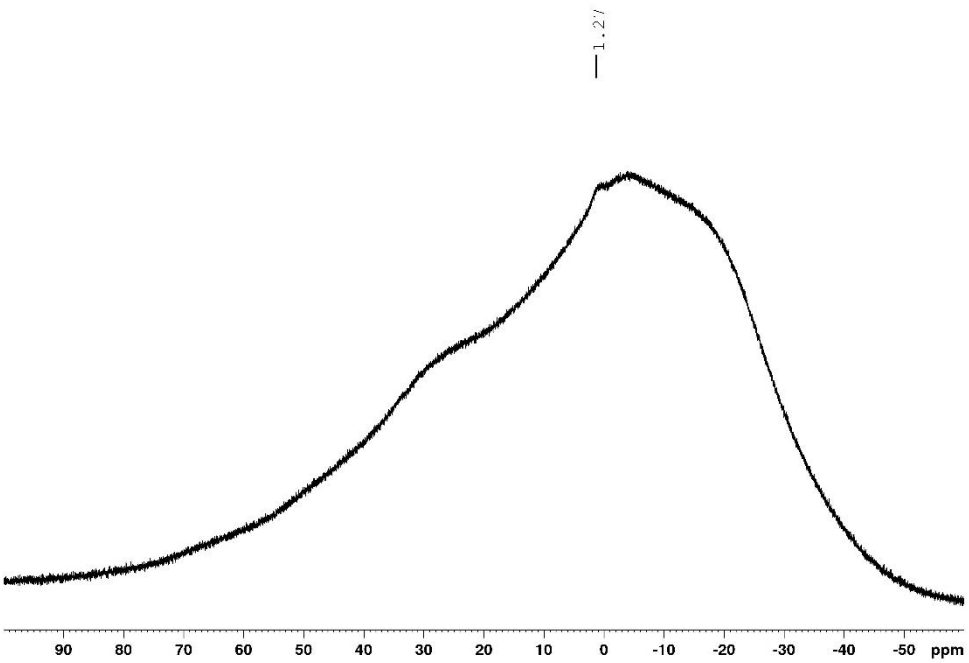

Figure S12. $^{11}B\{^{1}H\}$ NMR spectrum of compound **2** in d_8-THF at 128 MHz.

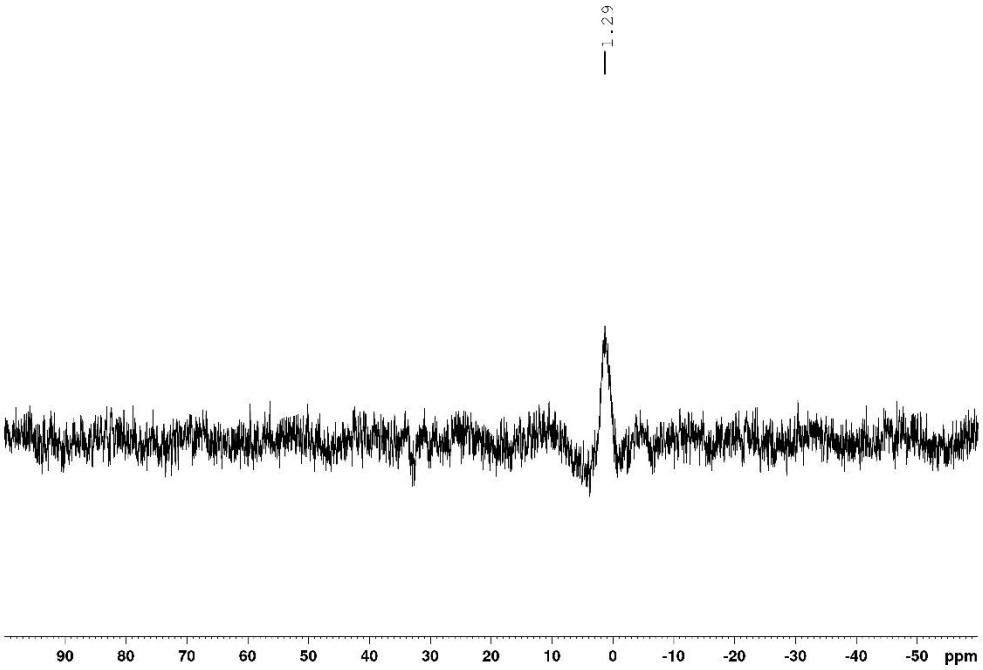

Figure S13. $^{11}B\{^{1}H\}$ NMR spectrum of compound **2** in d_8-THF at 128 MHz with background removed by linear backwards prediction.

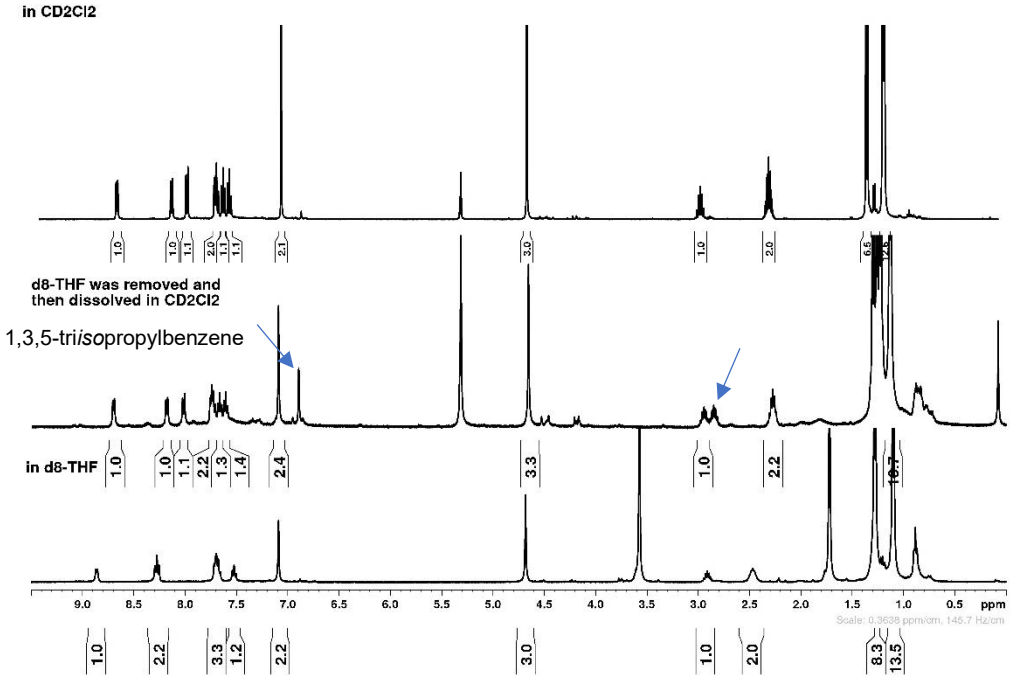

Figure S14. ^{1}H NMR spectra of compound **2** in d_8-THF (bottom), after d_8-THF was removed and the solid was re-dissolved in CD_2Cl_2 (middle) and in CD_2Cl_2 (top) at 400 MHz. The 1,3,5-tri*iso*propylbenene (marked with arrows) in the middle spectrum formed from decomposition.

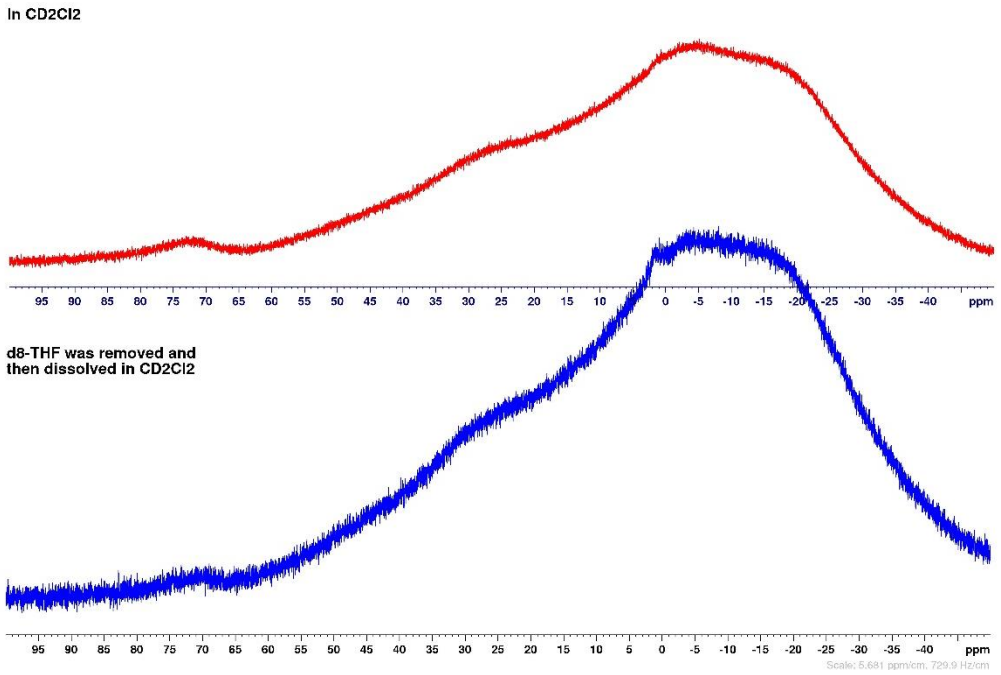

Figure S15. ^{11}B{^{1}H} NMR spectra of compound **2** in CD_2Cl_2 (top), and after the d_8-THF was removed and the solid was re-dissolved in CD_2Cl_2 (bottom) at 128 MHz.

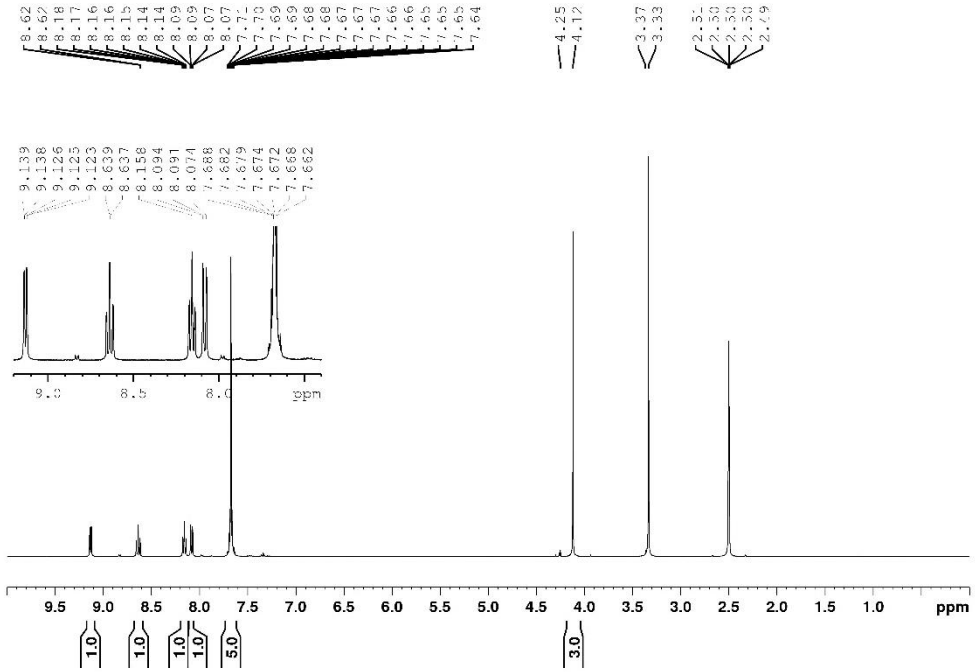

Figure S16. ^{1}H NMR spectrum of compound **3** in d_6-DMSO at 400 MHz.

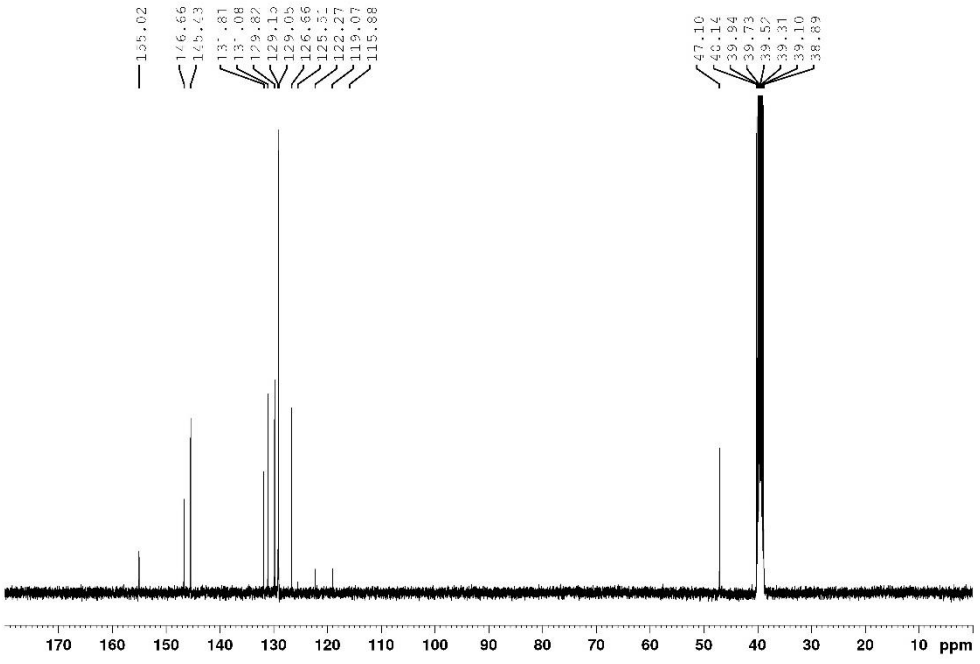

Figure S17. ^{13}C{^{1}H} NMR spectrum of compound **3** in d_6-DMSO at 100 MHz.

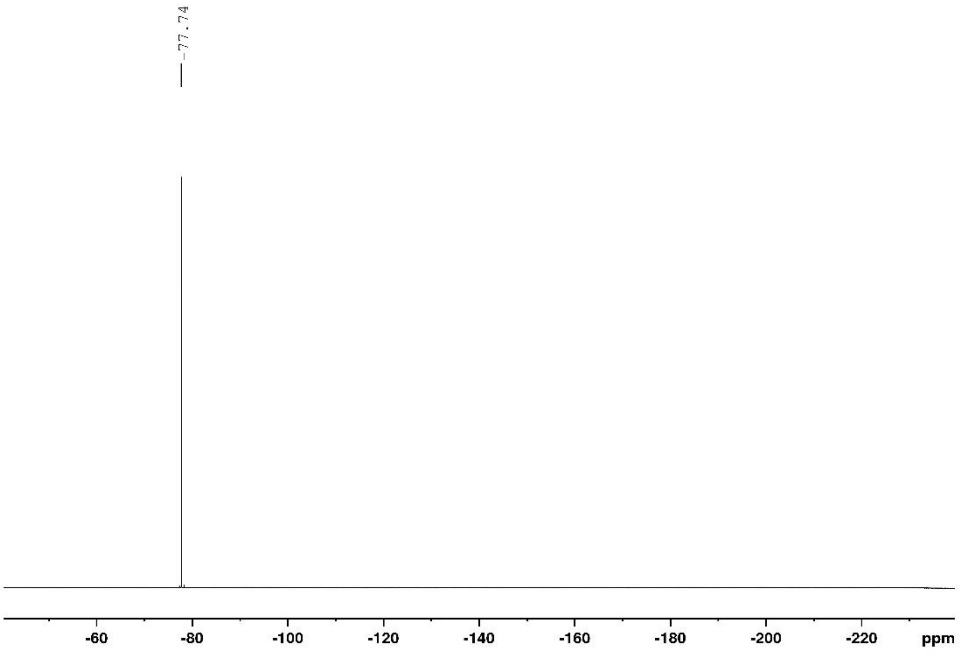

Figure S18. $^{19}F\{^{1}H\}$ NMR spectrum of compound **3** in d_6-DMSO at 376 MHz.

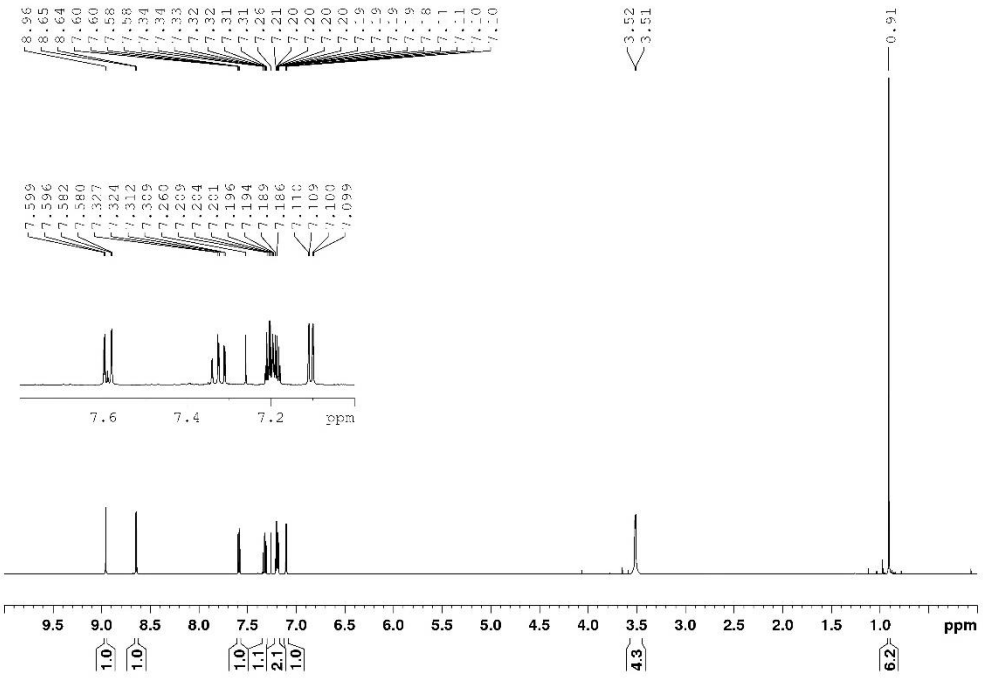

Figure S19. ^{1}H NMR spectrum of compound **5** in $CDCl_3$ at 500 MHz.

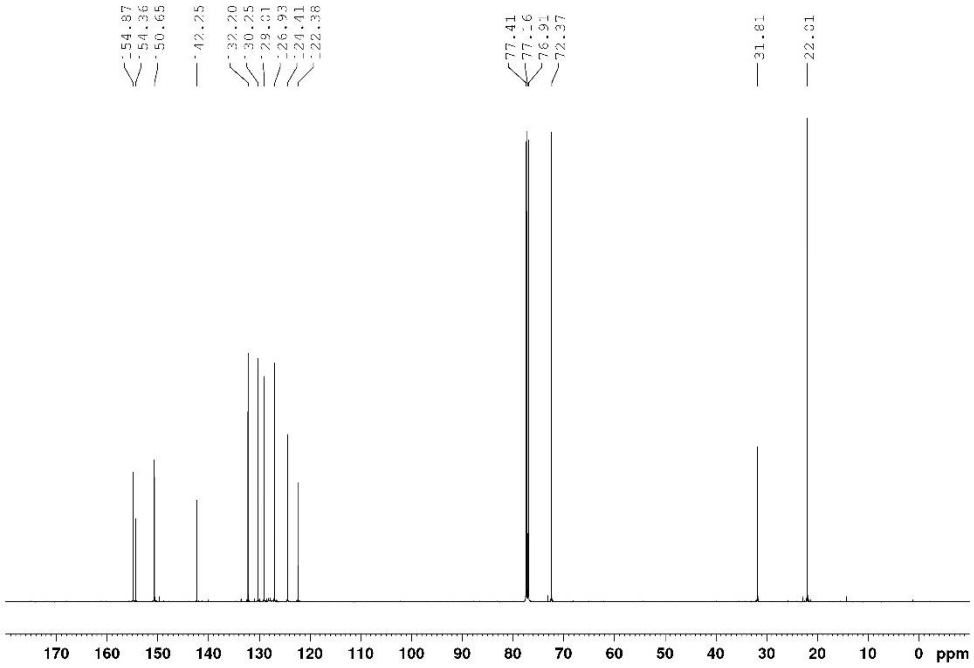

Figure S20. $^{13}C\{^{1}H\}$ NMR spectrum of compound **5** in $CDCl_3$ at 125 MHz.

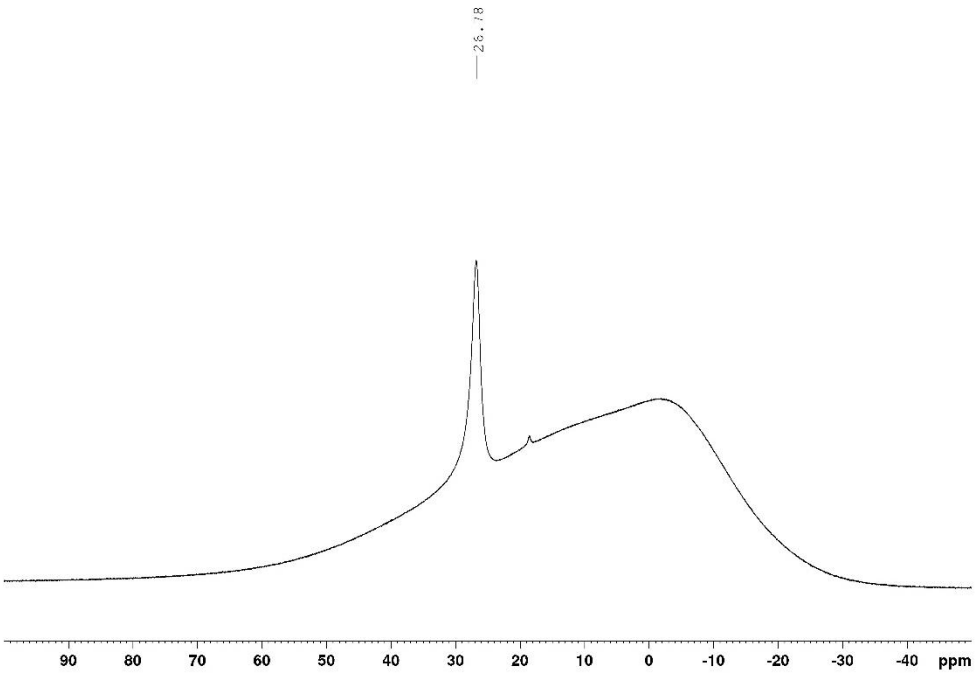

Figure S21. $^{11}B\{^{1}H\}$ NMR spectrum of compound **5** in $CDCl_3$ at 128 MHz.

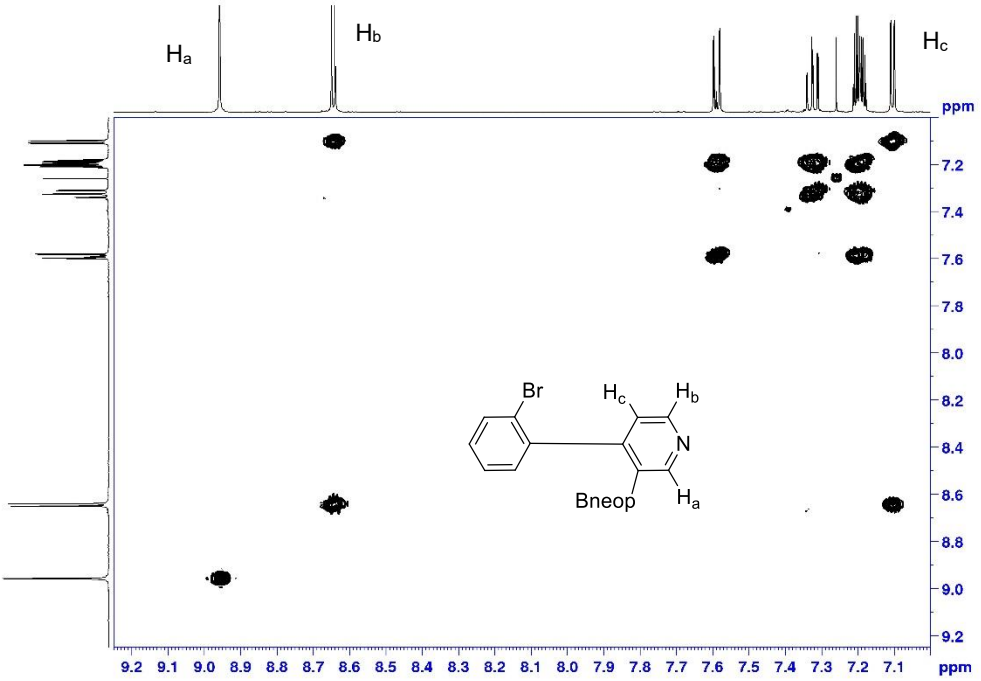

Figure S22. ^{1}H-^{1}H COSY spectrum of compound **5** in $CDCl_3$ at 500 MHz.

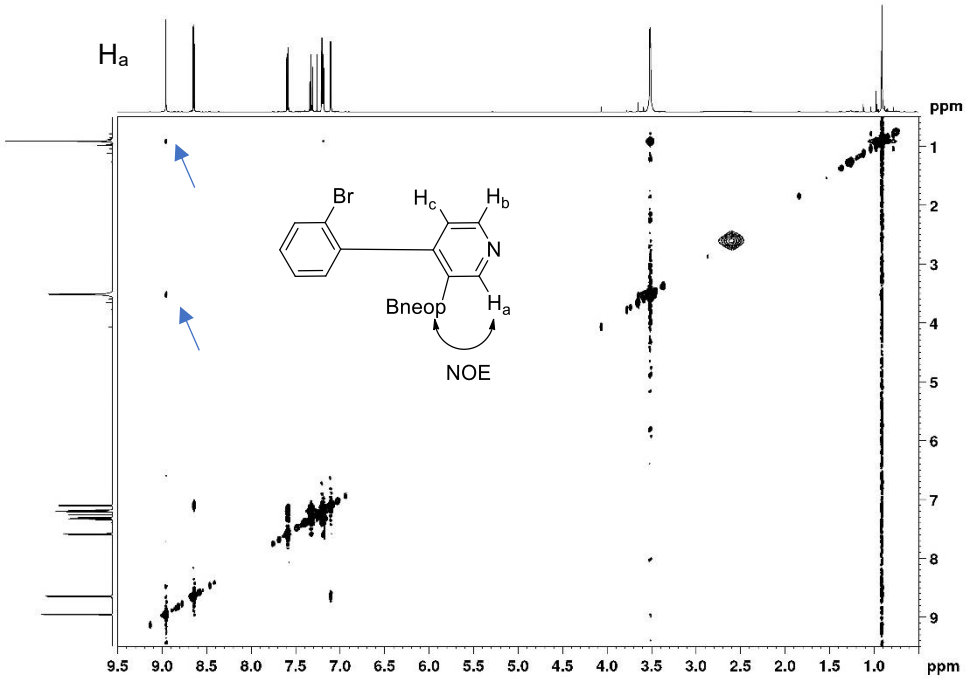

Figure S23. ^{1}H-^{1}H NOESY spectrum of compound **5** in $CDCl_3$ at 500 MHz.

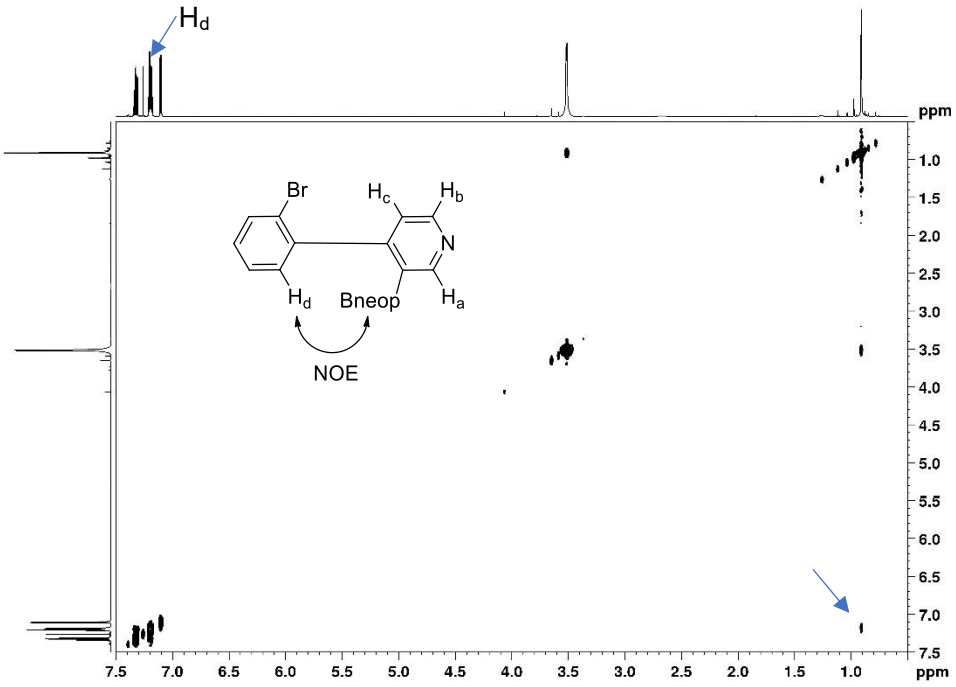

Figure S24. ^{1}H-^{1}H NOESY spectrum of compound **5** in $CDCl_3$ at 500 MHz.

Cyclic voltammetry

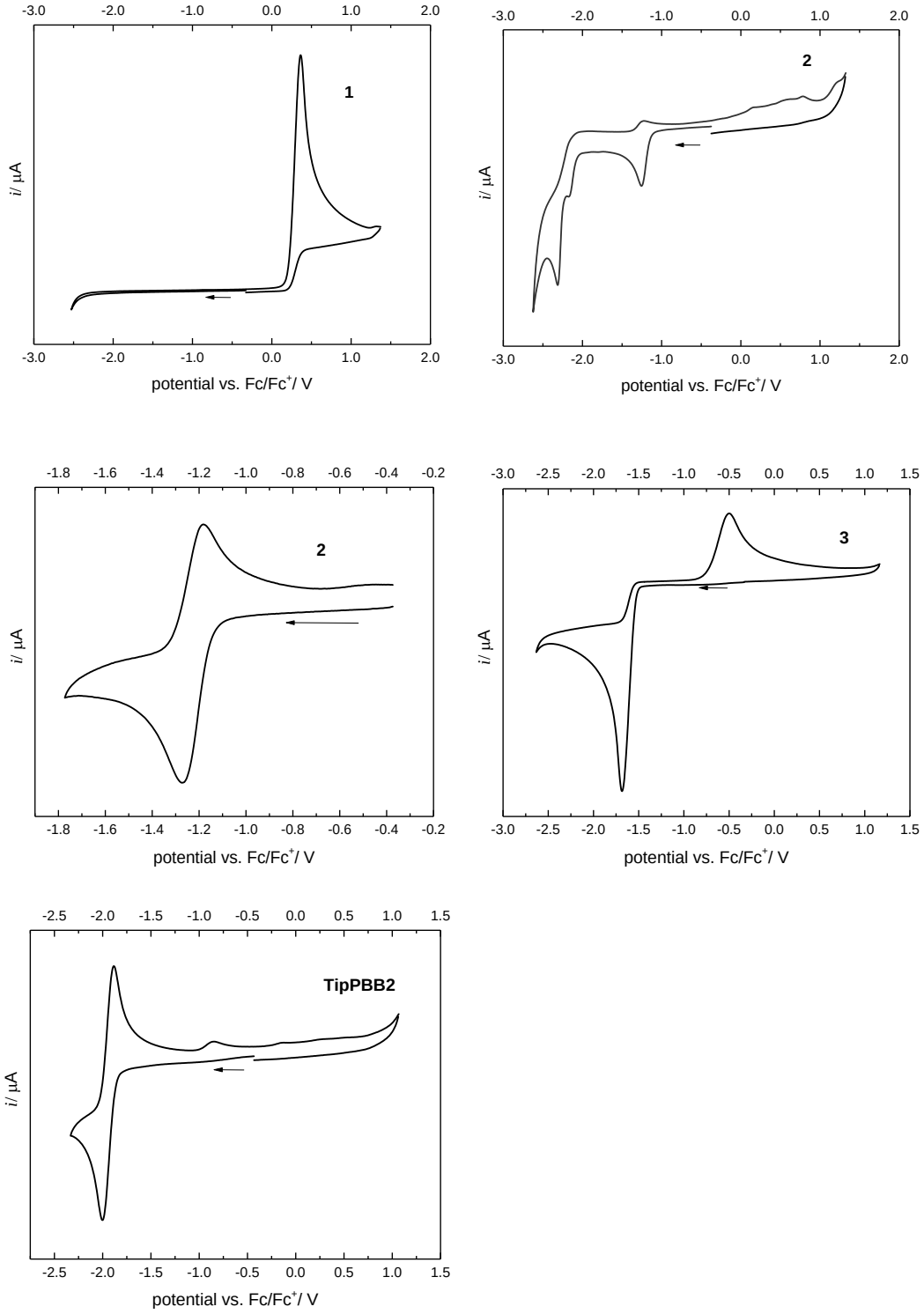

Figure S25. Cyclic voltammograms of compounds **1**, **2**, **3** and **TipPBB2**. Measured in CH_2Cl_2 in the presence of $TBAPF_6$ (0.1 M), scan rates of 250 mV s^{-1} with potentials given vs. the ferrocene/ferrocenium (Fc/Fc^+) couple.

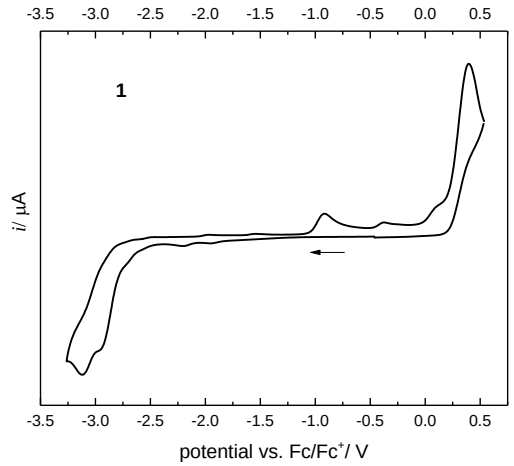

Figure S26. Cyclic voltammogram of compound **1**. Measured in THF in the presence of $TBAPF_6$ (0.1 M), scan rates of 250 mV s^{-1} with potentials given vs. the ferrocene/ferrocenium (Fc/Fc^+) couple.

TD-DFT Calculations

NICS values

NICS values were calculated at the B3LYP/6-311+G(d, p) level of theory. Dummy atoms were added to the optimized structures at the center of the borole ring, as well as 1 and 2 Å above and below the centre of the ring. $NICS(1)_{zz}$ values were taken from the zz component of the dummy atoms 1 Å above and below the borole ring. To verify the results the $NICS(1)_{zz}$ value, benzene was determined at the same level of theory and compared to previously published results ($NICS(1)_{zz}$ = –29.1; reported: –29.2).[10]

Compound	$NICS(1)_{zz}$	$NICS(1)_{zz}$ reported
1	–1.9	
2	16.4	
TipPBB2	21.2	
Benzene	–29.1	–29.2

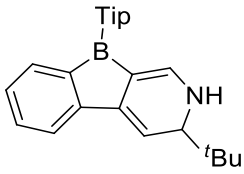

(**1**)

Calculated absorption spectra	Orbital	Energy [eV]
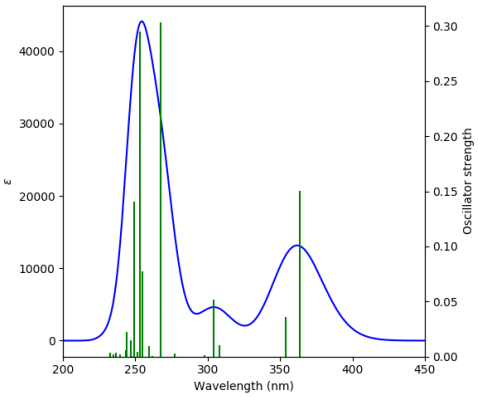	L+4	0.07
	L+3	0.01
	L+2	-0.46
	L+1	-1.18
	LUMO	-1.47
	HOMO	-5.33
	H-1	-5.98
	H-2	-6.15
	H-3	-6.22
TD-DFT B3LYP/6-31+G(d, p), gas phase	H-4	-6.83
Orbitals relevant to the $S_1 \leftarrow S_0$ transition	other relevant orbitals	
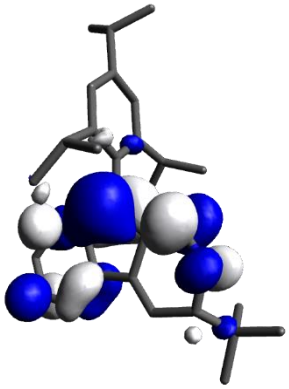 **LUMO**	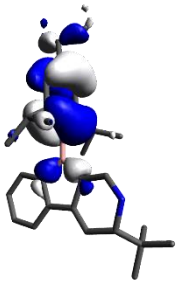 **HOMO-1**	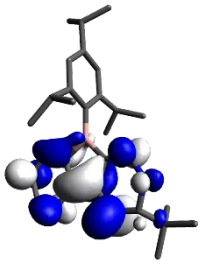 **LUMO+1**
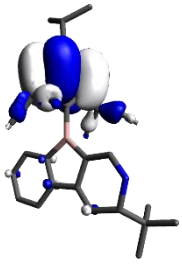 **HOMO-2**	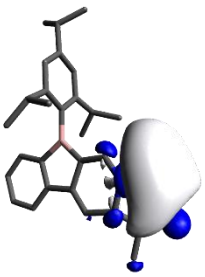 **LUMO+2**
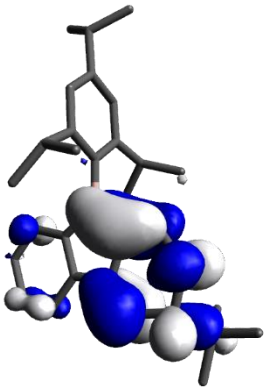 **HOMO**	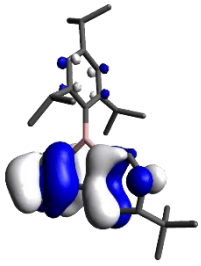 **HOMO-3**	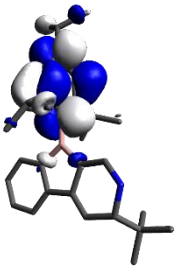 **LUMO+3**

Table S1: Lowest energy singlet electronic transition of compound **1** (TD-DFT B3LYP/6-31+G(d, p), gas phase).

State	E [eV]	λ [nm]	*f*	Symmetry	Major contributions	Λ
1	3.41	363.49	0.1505	A	HOMO->LUMO (91%)	0.66
2	3.50	353.91	0.0358	A	HOMO->L+1 (95%)	0.67
3	3.72	333.31	0.0001	A	H-1->LUMO (98%)	0.22
4	4.02	308.30	0.0103	A	H-2->LUMO (94%)	0.24
5	4.08	304.11	0.052	A	H-3->LUMO (86%)	0.58
6	4.16	298.06	0.0016	A	HOMO->L+2 (98%)	0.27
7	4.21	294.48	0.0001	A	H-1->L+1 (99%)	0.15
8	4.48	277.04	0.0029	A	H-2->L+1 (97%)	0.25
9	4.63	267.73	0.3035	A	H-4->L (35%), H-3->L+1 (50%)	0.72
10	4.73	261.98	0.0003	A	HOMO->L+3 (97%)	0.18
11	4.78	259.45	0.0097	A	HOMO->L+5 (89%)	0.26
12	4.86	255.13	0.0773	A	H-4->LUMO (14%), H->L+6 (60%)	0.33
13	4.90	252.88	0.2951	A	H-4->L (25%), H-3->L+1 (19%), HOMO->L+6 (31%)	0.49
14	4.93	251.29	0.004	A	HOMO->L+4 (82%)	0.17
15	4.98	249.19	0.1408	A	H-4->L+1 (45%), H->L+8 (22%)	0.58
16	5.01	247.52	0.0005	A	H-2->L+3 (41%), H-1->L+6 (43%)	0.64
17	5.02	246.77	0.0147	A	HOMO->L+7 (63%), H->L+8 (17%)	0.40
18	5.08	244.05	0.0225	A	H-1->L+2 (91%)	0.09
19	5.09	243.49	0.0056	A	H-4->L (12%), H-4->L+1 (32%), H->L+8 (40%)	0.54
20	5.18	239.52	0.0023	A	H->L+9 (67%), HOMO->L+12 (18%)	0.21
21	5.24	236.49	0.0032	A	H-3->L+2 (53%), H-2->L+2 (42%)	0.15
22	5.27	235.08	0.0022	A	H-3->L+2 (41%), H-2->L+2 (53%)	0.14
23	5.33	232.80	0.0019	A	HOMO->L+9 (16%), HOMO->L+12 (42%), HOMO->L+13 (15%)	0.23
24	5.33	232.50	0.0039	A	H-5->LUMO (80%)	0.35
25	5.34	232.39	0.0034	A	H->L+10 (63%), H->L+12 (13%)	0.25

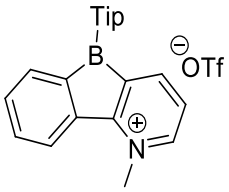

(**2**)

Calculated absorption spectra	Orbital	Energy [eV]
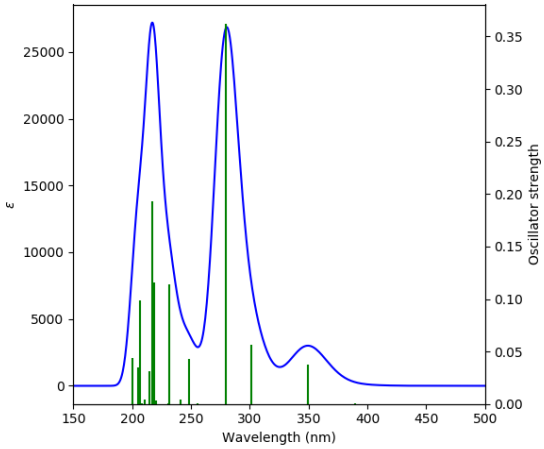	L+4	-2.10
	L+3	-2.53
	L+2	-2.86
	L+1	-4.69
	LUMO	-4.97
	HOMO	-10.18
	H-1	-10.23
	H-2	-11.45
	H-3	-11.91
TD-DFT CAM-B3LYP/6-31++G(d, p), gas phase	H-4	-12.24
Orbitals relevant to the $S_1 \leftarrow S_0$ transition	other relevant orbitals	
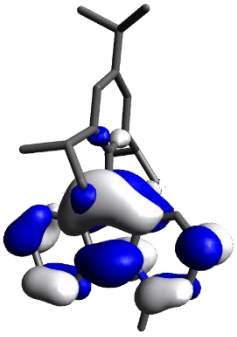 **LUMO**	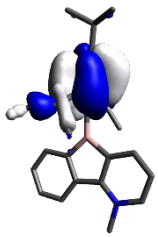 **HOMO-1**	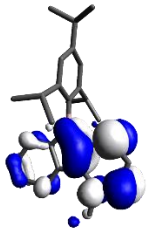 **LUMO+1**
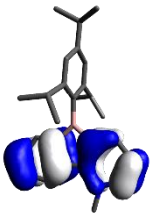 **HOMO-2**	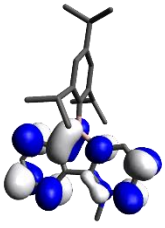 **LUMO+2**
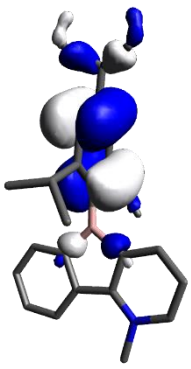 **HOMO**	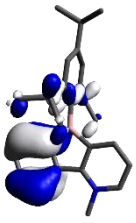 **HOMO-3**	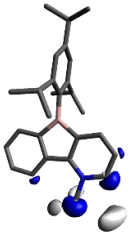 **LUMO+3**

Table S2: Lowest energy singlet electronic transition of compound **2** (TD-DFT CAM-B3LYP/6-31++G(d, p), gas phase).

State	E [eV]	λ [nm]	*f*	Symmetry	Major contributions	Λ
1	2.78	445.31	0	A	H->L (73%), H->L+1 (14%)	0.17
2	3.19	389.20	0.0009	A	H-1->L (78%), H-1->L+1 (13%)	0.13
3	3.55	349.52	0.0376	A	H-2->L (84%)	0.67
4	3.55	349.26	0.0037	A	H->L (14%), H->L+1 (68%)	0.18
5	3.80	325.99	0.0001	A	H-1->L (14%), H-1->L+1 (79%)	0.10
6	4.11	301.31	0.0564	A	H-3->L (46%), H-2->L+1 (44%)	0.60
7	4.43	279.99	0.3624	A	H-3->L (43%), H-2->L+1 (46%)	0.59
8	4.85	255.63	0.0005	A	H-12->L (20%), H-4->L (51%)	0.23
9	5.00	248.14	0.0429	A	H-3->L+1 (93%)	0.41
10	5.15	240.87	0.0041	A	H-1->L+8 (28%), H-1->L+9 (13%), H-1->L+10 (11%), H->L+11 (27%)	0.47
11	5.30	233.83	0.0001	A	H-17->L (22%), H-16->L (10%), H-14->L (16%), H-6->L (17%)	0.29
12	5.36	231.30	0.1137	A	H-7->L (43%), H-5->L (30%)	0.31
13	5.37	230.80	0.0002	A	H->L+2 (84%)	0.14
14	5.64	220.02	0.003	A	H-1->L+2 (85%)	0.11
15	5.67	218.72	0.0018	A	H-4->L (11%), H-4->L+1 (61%)	0.17
16	5.68	218.47	0.116	A	H-13->L (12%), H-9->L (23%)	0.46
17	5.70	217.50	0.1933	A	H-2->L+2 (13%), H-1->L+11 (10%), H->L+8 (20%)	0.56
18	5.77	214.72	0.0314	A	H-9->L (13%), H-7->L+1 (11%), H-5->L (18%), H-2->L+2 (12%)	0.41
19	5.89	210.42	0.0045	A	H-14->L (14%), H-8->L (22%), H-6->L (33%)	0.20
20	5.96	208.03	0.0007	A	H-17->L+1 (20%), H-14->L+1 (12%), H-6->L+1 (20%)	0.24
21	6.00	206.66	0.0987	A	H-7->L+1 (22%), H-5->L+1 (32%), H-2->L+2 (15%)	0.38
22	6.02	206.00	0.0081	A	H-12->L (16%), H-10->L (18%), H-4->L (11%)	0.26
23	6.05	204.98	0.0346	A	H-15->L+1 (10%), H-13->L (38%), H-2->L+2 (10%)	0.60
24	6.18	200.59	0.0012	A	H-17->L (13%), H-10->L (40%)	0.25
25	6.20	200.03	0.0441	A	H-5->L+1 (12%), H-2->L+2 (11%), H->L+3 (19%), H->L+6 (11%)	0.31

Theoretical calculations: Cartesian coordinates

Compound **1**

DFT B3LYP/6-31+G(d, p), gas phase, S_0

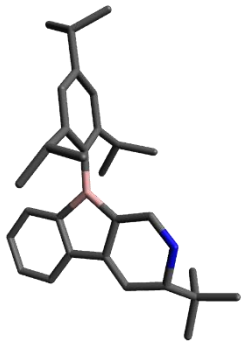

Point group: C_1

Total energy: –782,512.77 kcal mol^{-1}

Dipole moment: 3.97 D

Imaginary frequencies: 0

C	-0.43602100	4.35114800	-1.08834800
C	-1.83330300	4.38879800	-0.96051100
C	-2.53808700	3.26204900	-0.52988600
C	-1.83164000	2.09436700	-0.22514900
C	-0.41607000	2.03940800	-0.34722400
C	0.26716200	3.18323400	-0.78316300
C	-2.35762100	0.79261800	0.23563700
C	-1.21461500	-0.12276600	0.42401800
C	-3.62830600	0.42431100	0.48811100
C	-3.99645900	-0.97717500	0.92874800
N	-2.77353800	-1.75745700	1.20292900
C	-1.50747900	-1.35949600	0.92978200
C	-4.95440700	-1.73716300	-0.07098900
C	-6.26038700	-0.92973000	-0.21470100
C	-5.30497800	-3.12163700	0.51401200
C	-4.29077300	-1.90856900	-1.44769400
H	0.09628800	5.23625800	-1.42634000
H	-2.37135900	5.30211700	-1.19990300
H	-3.62057300	3.30211300	-0.43639400
H	1.34982000	3.16191900	-0.88381300
H	-4.44936400	1.12769300	0.38952200
H	-4.56047600	-0.91299600	1.87543400
H	-2.90040700	-2.66245300	1.62911200
H	-0.73716100	-2.09236200	1.15839600
H	-6.09519900	0.02976100	-0.71336000
H	-6.98509500	-1.49010200	-0.81532500
H	-6.72100200	-0.73315700	0.76157800
H	-4.43401700	-3.78542000	0.56075700
H	-6.04741600	-3.62284500	-0.11632700
H	-5.73159800	-3.03650600	1.52167400
H	-4.96296000	-2.43973900	-2.13110100
H	-4.04826200	-0.93954600	-1.89471600
H	-3.36327500	-2.48581600	-1.37413200
B	0.08728400	0.60041700	0.07364500
C	1.58728100	0.09277800	0.11420200
C	2.39928000	0.26883700	1.27306300
C	2.19235900	-0.51431500	-1.02846600
C	3.75035400	-0.11533200	1.24517300
C	3.54707300	-0.87696900	-0.99634500
C	4.35488300	-0.68195700	0.12501700
H	4.35228700	0.03803100	2.13938100
H	3.97802100	-1.32800300	-1.88768100
C	1.46338000	-0.88704500	-2.33076100
H	2.26372000	-1.13234100	-3.04031700
C	0.62489300	-2.17369700	-2.17315500
H	1.22855200	-2.98827200	-1.75856200
H	-0.23014800	-2.00899000	-1.51162200
H	0.23888600	-2.49778600	-3.14744400
C	0.63937700	0.22341500	-3.00429600
H	-0.28746900	0.44443900	-2.46960600
H	1.20850000	1.15454900	-3.08586400
H	0.36122600	-0.09386400	-4.01650400
C	5.82844200	-1.06672500	0.13763700
H	6.21474000	-0.81251100	1.13402100
C	6.03412100	-2.58111200	-0.06255100
H	5.68552300	-2.90198800	-1.05086500
H	7.09625400	-2.84104700	0.01631100
H	5.48435200	-3.15775100	0.68866900
C	6.64444800	-0.26027300	-0.89177100
H	6.52997400	0.81668500	-0.73086300
H	7.71040700	-0.50609200	-0.81910300
H	6.32028700	-0.48101800	-1.91522800
C	1.91815700	0.79891500	2.63500900
H	2.83814400	0.98461500	3.20354400
C	1.13739900	-0.27127400	3.42776000
H	0.17018100	-0.47988600	2.96205800
H	1.70137200	-1.20848400	3.48591300

H	0.94825400	0.07630500	4.45078700
C	1.15730500	2.13549200	2.63095900
H	1.67881300	2.89486200	2.04037600
H	0.14339400	2.04260700	2.23475100
H	1.07052100	2.50631500	3.65934000

Compound 2

DFT B3LYP/6-31+G(d, p), gas phase, S_0

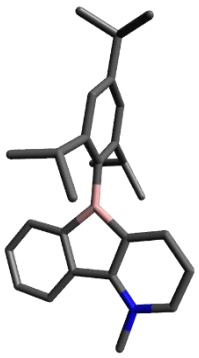

Point group: C_1

Total energy: –707,987.61 kcal mol^{-1}

Dipole moment: 12.43 D

Imaginary frequencies: 0

C	2.47565800	3.52052500	-0.20781100
C	3.77866900	3.02497000	-0.24028000
C	4.03069500	1.64533700	-0.18858900
C	2.95118100	0.75969200	-0.10309700
C	1.61305900	1.25924400	-0.06965700
C	1.39239900	2.63332100	-0.12234200
C	2.90065600	-0.72234400	-0.03341600
C	1.56738700	-1.19392700	0.04405400
N	3.93194200	-1.61091400	-0.03580400
C	3.67761000	-2.95766800	0.03690000
C	2.39819200	-3.45385300	0.11347100
C	1.31744400	-2.55293600	0.11722800
C	5.34628400	-1.18589500	-0.11453200
H	2.30279900	4.59133800	-0.24878300
H	4.61682400	3.71143400	-0.30654500
H	5.06067900	1.31949900	-0.21718700
H	0.37689000	3.01720700	-0.09695500
H	4.54893500	-3.59956600	0.02990200
H	2.25159900	-4.52637700	0.16907700
H	0.29604800	-2.91769600	0.17690400
H	5.97796000	-2.07201300	-0.10060500
H	5.51631400	-0.64120300	-1.04427000
H	5.59133600	-0.55961700	0.74438600
B	0.58886100	0.07054100	0.02711400
C	-0.97085100	0.04099500	0.09382700
C	-1.65302300	0.05193700	1.34676300

C	-1.75723400	-0.06011600	-1.09549100	H	-0.14947800	2.28914900	2.31681800
C	-3.04764900	-0.09235700	1.37640300	H	-1.83047400	2.32459800	2.86906100
C	-3.14688500	-0.20114500	-0.99787700	H	-0.52527500	1.98858700	4.01985300
C	-3.82113800	-0.23309100	0.22499800	C	0.33212400	-0.41025300	2.97802700
H	-3.54665300	-0.09287100	2.34321500	H	0.26586100	-1.48603900	2.78931900
H	-3.71747200	-0.28647600	-1.91931800	H	1.15528500	0.00240200	2.38062100
C	-1.21643100	0.06630200	-2.52619800	H	0.62368700	-0.27056700	4.02462600
H	-1.98048900	-0.38795400	-3.16812300	C	-5.33100700	-0.40625500	0.30849400
C	-1.10979100	1.54711100	-2.95171800	H	-5.59503100	-0.38499500	1.37376600
H	-2.05714100	2.07084000	-2.79461300	C	-6.08181600	0.75218500	-0.37730700
H	-0.33655300	2.07160700	-2.38077400	H	-7.16234600	0.63964900	-0.23987100
H	-0.85084200	1.62375100	-4.01361600	H	-5.78572000	1.72103400	0.03765100
C	0.08782100	-0.67960900	-2.83559600	H	-5.88595300	0.77317100	-1.45527700
H	0.95763000	-0.22028400	-2.34862400	C	-5.78249100	-1.76895800	-0.25322200
H	0.03782100	-1.73323600	-2.54457400	H	-5.56926100	-1.84881700	-1.32518200
H	0.29142600	-0.63790200	-3.91109200	H	-5.27644100	-2.59717000	0.25357400
C	-0.99872900	0.30451700	2.71152300	H	-6.86171000	-1.89775600	-0.11960200
H	-1.70469900	-0.09111500	3.45133100				
C	-0.86937400	1.81745100	2.99377200				

References

1 S. -F. Liu, Q. Wu, H. L. Schmider, H. Aziz, N. -X. Hu, Z. Popović and S. Wang, *J. Am. Chem. Soc.*, 2000, **122**, 3671.

2 M. J. Frisch, G. W. Trucks, H. B. Schlegel, G. E. Scuseria, M. A. Robb, J. R. Cheeseman, G. Scalmani, V. Barone, B. Mennucci, G. A. Petersson, H. Nakatsuji, M. Caricato, X. Li, H. P. Hratchian, A. F. Izmaylov, J. Bloino, G. Zheng, J. L. Sonnenberg, M. Hada, M. Ehara, K. Toyota, R. Fukuda, J. Hasegawa, M. Ishida, T. Nakajima, Y. Honda, O. Kitao, H. Nakai, T. Vreven, J. A. Montgomery, J. E. Peralta, F. Ogliaro, M. Bearpark, J. J. Heyd, E. Brothers, K. N. Kudin, V. N. Staroverov, R. Kobayashi, J. Normand, K. Raghavachari, A. Rendell, J. C. Burant, S. S. Iyengar, J. Tomasi, M. Cossi, N. Rega, J. M. Millam, M. Klene, J. E. Knox, J. B. Cross, V. Bakken, C. Adamo, J. Jaramillo, R. Gomperts, R. E. Stratmann, O. Yazyev, A. J. Austin, R. Cammi, C. Pomelli, J. W. Ochterski, R. L. Martin, K. Morokuma, V. G. Zakrzewski, G. A. Voth, P. Salvador, J. J. Dannenberg, S. Dapprich, A. D. Daniels, Farkas, J. B. Foresman, J. V. Ortiz, J. Cioslowski and D. J. Fox, Revision A.03 ed., Gaussian Inc., Wallingford CT, 2016.

3 M. D. Hanwell, D. E. Curtis, D. C. Lonie, T. Vandermeersch, E. Zurek and G. R. Hutchison, *J. Cheminformatics*, 2012, **4**, 17.

4 T. Lu and F. Chen, *J. Comput. Chem.*, 2012, **33**, 580592.

5 C. Lee, W. Yang and R. G. Parr, *Phys. Rev. B: Condens. Matter Mater. Phys.*, 1988, **37**, 785.

6 (*a*) G. A. Petersson and M. A. Al-Laham, *J. Chem. Phys.*, 1991, **94**, 6081; (*b*) G. A. Petersson, A. Bennett, T. G. Tensfeldt, M. A. Al-Laham, W. A. Shirley, J. Mantzaris and *J. Chem. Phys.*, 1988, **89**, 2193.

7 S. Durben and T. Baumgartner, *Inorg. Chem.*, 2011, **50**, 6823.

8 J. J. Murphy, D. Bastida, S. Paria, M. Fagnoni and P. Melchiorre, *Nature*, 2016, **532**, 218.

9 K. Leduskrasts and E. Suna, *RSC Adv.*, 2019, **9**, 460.

10 N. S. Mills, K. B. Llagostera, *J. Org. Chem.*, 2007, **72**, 9163.